MTOpen

Targeted Gene Delivery to the Enteric Nervous System Using AAV: A Comparison Across Serotypes and Capsid Mutants

Matthew J Benskey[1,2], Nathan C Kuhn[1], James J Galligan[2,3], Joanna Garcia[1], Shannon E Boye[4], William W Hauswirth[4], Christian Mueller[5], Sanford L Boye[4] and Fredric P Manfredsson[1,2]

[1]Department of Translational Science and Molecular Medicine, College of Human Medicine, Michigan State University, Grand Rapids, Michigan, USA; [2]Neuroscience Program, Michigan State University, East Lansing, Michigan, USA; [3]Department of Pharmacology and Toxicology, Michigan State University, East Lansing, Michigan, USA; [4]Department of Ophthalmology, University of Florida, Gainesville, Florida, USA; [5]Department of Pediatrics, University of Massachusetts Medical School, Worcester, Massachusetts, USA

Recombinant adeno-associated virus (AAV) vectors are one of the most widely used gene transfer systems in research and clinical trials. AAV can transduce a wide range of biological tissues, however to date, there has been no investigation on targeted AAV transduction of the enteric nervous system (ENS). Here, we examined the efficiency, tropism, spread, and immunogenicity of AAV transduction in the ENS. Rats received direct injections of various AAV serotypes expressing green fluorescent protein (GFP) into the descending colon. AAV serotypes tested included; AAV 1, 2, 5, 6, 8, or 9 and the AAV2 and AAV8 capsid mutants, AAV2-Y444F, AAV2-tripleY-F, AAV2-tripleY-F+T-V, AAV8-Y733F, and AAV8-doubeY-F+T-V. Transduction, as determined by GFP-positive cells, occurred in neurons and enteric glia within the myenteric and submucosal plexuses of the ENS. AAV6 and AAV9 showed the highest levels of transduction within the ENS. Transduction efficiency scaled with titer and time, was translated to the murine ENS, and produced no vector-related immune response. A single injection of AAV into the colon covered an area of ~47 mm^2. AAV9 primarily transduced neurons, while AAV6 transduced enteric glia and neurons. This is the first report on targeted AAV transduction of neurons and glia in the ENS.

INTRODUCTION

Recombinant adeno-associated virus (AAV) is one of the most widely used gene therapy systems in research and clinical trials.[1–3] AAV is favored over other viral vectors due to its lack of pathogenicity and the ability to establish expression within both dividing and mature nondividing cells of multiple lineages. Further, AAV vectors can achieve high levels of transduction within weeks that are maintained over the lifetime of an organism.[2,4] AAV vectors can efficiently transduce many different biological tissues including; muscle, liver, brain, lung, and retina (reviewed in ref. 4). Although there have been reports that AAV can transduce cells of the gut following systemic or peroral delivery,[5–7] to date, there has been no focused investigation on the ability of AAV to directly transduce cells of the enteric nervous system (ENS) following targeted injections.

The ENS is a division of the autonomic nervous system. The ENS coordinates control of enterocyte secretion, nutrient and fluid absorption, blood flow, and motor function in the gastrointestinal (GI) system. The ENS consists of an estimated 100 million neurons, which are embedded in the gut wall, spanning from the esophagus to the anus. These neurons are organized into ganglia located in either the myenteric plexus (MP) or submucosal plexus (SMP). The myenteric plexus is located between the circular and longitudinal muscle, while the submucosal plexus is located just below the mucosa in the lumen of the gut. Although the ENS is connected to the CNS, the ENS is composed of integrative neuronal circuits, which can control most gut functions independent of CNS connections.[8]

Abnormalities of the ENS cause disruptions in GI function that manifest in functional disorders such as gastroparesis, irritable bowel syndrome, Allgrove syndrome, hypertrophic pyloric stenosis, Hirschprung disease, or intestinal neuronal dysplasia.[2] Many of these disorders are not life threatening but they do cause extreme patient discomfort and reduced quality of life.[9] However, in some instances, the etiological root of a disease may begin in the ENS and spread to other areas of the body. For example, GI dysfunction shows a high degree of comorbidity with Parkinson's disease (PD), and the hypothesis that PD pathology originates in the gut has gained support.[10–13] As such, the ENS has garnered increased attention in the study of neurodegenerative disease.

Currently, available model systems for studying disease and dysfunction of the ENS are lacking and rely heavily on the use of psychological stress, toxicants, or transgenic animals.[14] However, due to the inherent shortcomings of these model systems (*e.g.*, the presence of off target effects due to systemically delivered agents or developmental compensations associated with germline mutations),[15–17] a more elegant and effective way to study ENS function or dysfunction is needed. Accordingly, the ability of AAV to transduce cells of adult animals offers a large advantage over other

Correspondence: Fredric Manfredsson, Department of Translational Science and Molecular Medicine, College of Human Medicine, Michigan State University, 333 Bostwick Ave NE, Grand Rapids, Michigan, USA. E-mail: Fredric.manfredsson@hc.msu.edu

transgenic animal models. Furthermore, targeted use of AAV allows for both spatial and temporal control of genetic overexpression or knockdown, which could be used to model and potentially treat ENS dysfunction in discrete areas, or even phenotypically distinct cell types, of the GI system.

Although AAV vectors hold great potential for studying both the function and dysfunction of the ENS, to date little is known about the transduction profile of AAV in the ENS. The purpose of the current study was to examine the ability of various AAV serotypes to infect cells of the ENS. Adult rats received direct injections of AAV expressing green fluorescent protein (GFP) into the wall of the descending colon. We compared the transduction efficiencies of wild-type (WT) AAV serotypes 1, 2, 5, 6, 8, or 9 as well as several capsid mutants based on AAV2 and AAV8 vectors, which have exhibited increased transduction in other organs.[18–22] The time- and titer-dependent efficiency, tropism, and spread of AAV transduction as well as any inflammatory response were evaluated within the MP and SMP. Finally, we investigated the ability to translate the current technique to other areas of the GI tract and other species.

RESULTS

Transduction efficiency of AAV in the ENS

In order to determine the transduction efficiency of various serotypes of AAV in the ENS, adult rats received direct injections of AAV expressing GFP under the control of the hybrid chicken β-actin/cytomegalovirus promoter into the wall of the descending colon. One month following injection, GFP-positive cells were quantified and used as an index of transduction efficiency. All unmodified WT serotypes tested exhibited some expression within the ENS; however, there was differential transduction efficiency between serotypes. Within the MP, AAV1 (2.8 ± 1.6 cells/mm²; **Figure 1a,c**) and AAV2 (3.3 ± 1.4 cells/mm²; **Figure 1a,d**) showed low levels of expression. In contrast, AAV6 (16.4 ± 3.6 cells/mm²; **Figure 1a,f**) and AAV9 (15.7 ± 2.5 cells/mm²; **Figure 1a,h**) showed the highest levels of expression

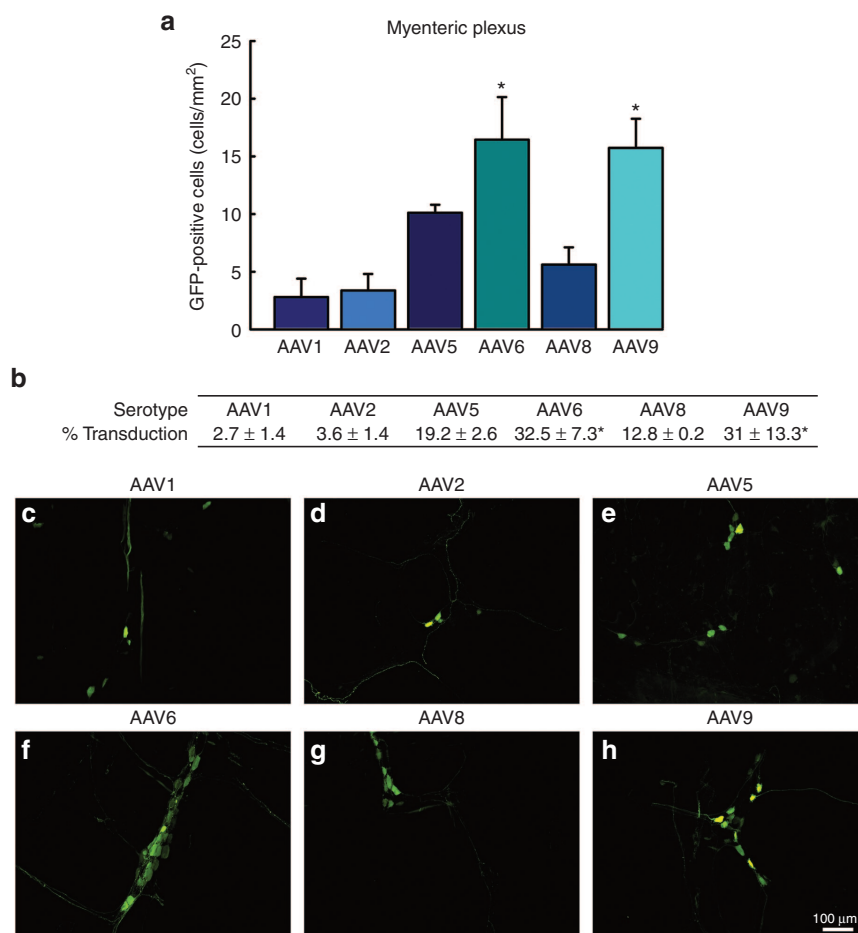| Serotype	AAV1	AAV2	AAV5	AAV6	AAV8	AAV9
% Transduction	2.7 ± 1.4	3.6 ± 1.4	19.2 ± 2.6	$32.5 \pm 7.3*$	12.8 ± 0.2	$31 \pm 13.3*$

Figure 1 Transduction efficiency of recombinant adeno-associated virus (AAV) in the myenteric plexus (MP) of the enteric nervous system: a comparison across serotypes 1, 2, 5, 6, 8, and 9. Adult male rats received direct injections of AAV (6×5 μl injections at 1.3×10^{12} vg/ml) into the wall of the descending colon and were sacrificed one month later, at which time the MP was dissected and native fluorescence was viewed under a fluorescent microscope. (**a**) Transduction efficiency of AAV1, 2, 5, 6, 8, and 9, was measured by the quantification of green fluorescent protein (GFP) expressing cells in the MP. Columns represent mean number of GFP-positive cells, expressed as cells/mm², + 1 SEM ($n = 4$–6/group). AAV6 and 9 exhibited significantly greater numbers of GFP positive cells than AAV1 and AAV2. (**b**) The percent of HUc-positive cells transduced for each respective serotype. Table represents percent of HUc cells colocalized with GFP ± SEM ($n = 4$–6/group). (**c–h**) Shows representative images of GFP-positive cells in the MP following transduction by AAV1, 2, 5, 8, and 9. Scale bar in (**h**) represents 100 μm and applies to panels (**c–g**). * Indicates significantly different than AAV1 and AAV2 ($P < 0.05$).

and exhibited significantly more GFP-positive cells than AAV1 and AAV2. AAV5 (10.1 ± 0.7 cells/mm²; **Figure 1a,e**) and AAV8 (5.6 ± 1.4 cells/mm²; **Figure 1a,g**) showed moderate expression, however there were no significant changes in GFP cell number associated with these groups. In addition to quantifying the number of GFP-positive cells/mm², the percent of HUc (a pan neuronal marker) positive cells transduced within the injected area were also quantified. The serotype dependent changes in the percent of HUc-positive cells transduced in the MP roughly mirrored changes in GFP-positive cells/mm², with AAV1 ($2.7 \pm 1.4\%$) and AAV2 ($3.6 \pm 1.4\%$) transducing a low percent of neurons within the MP (**Figure 1b**). AAV6 ($32.5 \pm 7.3\%$) and AAV9 ($31 \pm 13.3\%$) transduced a significantly higher percent of HUc positive neurons in the MP than AAV1 and AAV2 (**Figure 1b**). Finally, AAV5 ($19.2 \pm 2.6\%$) and AAV8 ($12.8 \pm 0.2\%$) transduced an intermediated proportion of neurons in the MP, and showed no significant differences from other serotypes examined.

A similar pattern of transduction was observed within the SMP, and there were no differences in the transduction efficiency between the MP and SMP. AAV1 (3.9 ± 1.2 cells/mm²; **Figure 2a,c**) and AAV2 (2.8 ± 1.1 cells/mm²; **Figure 2a,d**) displayed low levels of transduction with sparse GFP-positive cells throughout the SMP. Again, AAV6 (14.7 ± 4.6 cells/mm²; **Figure 2a,f**) and AAV9 (11.9 ± 1.7 cells/mm²; **Figure 2a,h**) showed the highest level of transduction and had significantly greater numbers of GFP-positive cells than AAV1 and AAV2. Within the SMP, AAV5 (9.1 ± 2.2 cells/mm²; **Figure 2a,e**) and AAV8 (5 ± 1.8 cells/mm²; **Figure 2a,g**) displayed moderate levels of expression similar to that observed in the MP. Within the SMP, the changes observed between serotypes in the number of GFP-positive cells/mm² were similar to the percent of neurons transduced. AAV6 ($36.4 \pm 15.2\%$) and AAV9 (32.8 ± 10.1) transduced significantly more HUc-positive cells than AAV1 ($7.9 \pm 2.9\%$) and AAV2 ($2.7 \pm 2.7\%$; **Figure 2b**). AAV5 ($21.8 \pm 5.2\%$) and AAV8

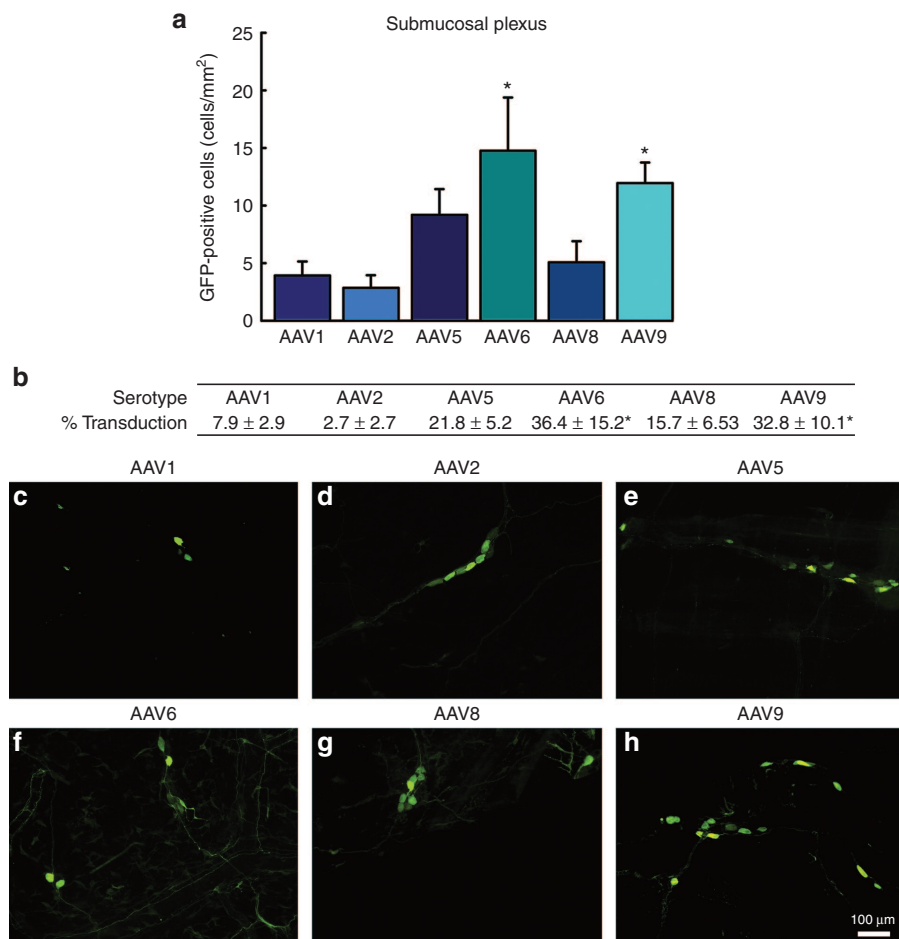| Serotype	AAV1	AAV2	AAV5	AAV6	AAV8	AAV9
% Transduction	7.9 ± 2.9	2.7 ± 2.7	21.8 ± 5.2	$36.4 \pm 15.2*$	15.7 ± 6.53	$32.8 \pm 10.1*$

Figure 2 Transduction efficiency of recombinant adeno-associated virus (AAV) in the submucosal plexus (SMP) of the enteric nervous system: a comparison across serotypes 1, 2, 5, 6, 8, and 9. Adult male rats received direct injections of AAV (6×5 µl injections at 1.3×10^{12} vg/ml) into the wall of the descending colon and were sacrificed one month later, at which time the SMP was dissected and viewed under a fluorescent microscope. (**a**) Transduction efficiency of AAV1, 2, 5, 6, 8, and 9 was measured by the quantification of green fluorescent protein (GFP) expressing cells in the SMP. Columns represent mean number of GFP-positive cells, expressed as cells/mm², + 1 SEM ($n = 4$–6/group). AAV6 and 9 exhibited significantly greater numbers of GFP-positive cells than AAV1 and AAV2. (**b**) The percent of HUc-positive cells transduced for each respective serotype. Table represents the percent of HUc cells colocalized with GFP ± SEM ($n = 4$–6/group). (**c**–**h**) Representative images of GFP-positive cells in the SMP following transduction by AAV1, 2, 5, and 9. Scale bar in (**h**) represents 100 µm and applies to panels (**c**–**g**). * Indicates significantly different than AAV1 and AAV2 ($P < 0.05$).
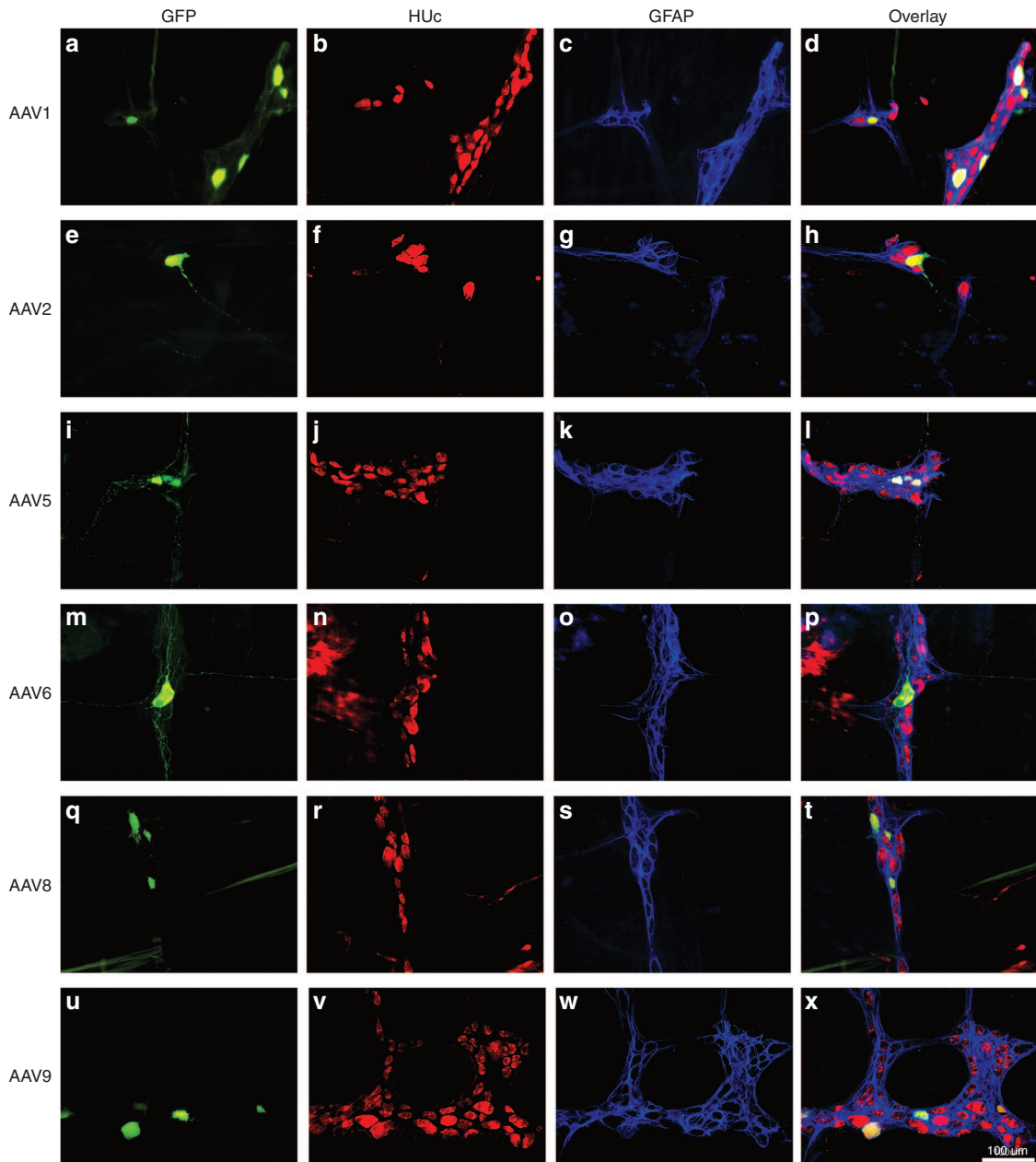
Figure 3 Neuronal tropism of recombinant adeno-associated virus (AAV) transduction in the myenteric plexus (MP): serotypes 1, 2, 5, 6, 8, and 9. Adult male rats received direct injections of AAV (6×5 µl injections at 1.3×10^{12} vg/ml) into the wall of the descending colon and were sacrificed one month later, at which time the MP was dissected. MP tissue was stained for the neuronal marker HUc (red) and the enteric glia marker, glial fibrillary acidic protein (GFAP; blue). Following the MP was viewed under a fluorescent microscope and the transduction of neurons in the MP was determined by examining the colocalization of green fluorescent protein (GFP; green) expression in HUc-positive cells (colocalization appears yellow). Neuronal transduction was observed for all serotypes examined. Representative images of neuronal transduction are shown for AAV1 (**a–d**), AAV2 (**e–h**), AAV5 (**i–l**), AAV6 (**m–p**), AAV8 (**q–t**), and AAV9 (**u–x**). Scale bar in (**x**) represents 100 µm and applies to panels (**a–w**).

(15.7 ± 6.53) transduced an intermediate percent of neurons compared to the other serotypes (**Figure 2b**).

We next compared the transduction of unmodified AAV serotypes to that of several AAV2- and AAV8-based capsid mutants. These capsid mutants showed no significant changes in the number of GFP-positive cells/mm² or the percent of neurons transduced in either the MP or the SMP, compared to their parent serotypes. AAV2-Y444F transduced 2.5 ± 2.5 cells/mm² in the MP (**Supplementary Figure S1a,d**) and 5.7 ± 2.1 cells/mm²

in the SMP (**Supplementary Figure S1g,j**) corresponding to 6.5 ± 6.5% of HUc cells in the MP (**Supplementary Figure S1b**) and 21.2 ± 6.7% of HUc-positive cells and SMP (**Supplementary Figure S1h**). AAV2-tripleY-F transduced 3.9 ± 1.4 cells/mm² in the MP (**Supplementary Figure S1a,e**) and 1.6 ± 0.6 cells/mm² in the SMP (**Supplementary Figure S1g,k**) corresponding to 5.8 ± 2.9% and 6.4 ± 2% of HUc-positive cells transduced in the MP and SMP, respectively (**Supplementary Figure S1b,h**). AAV2-tripleY-F+T-V transduced 8 ± 1.5 cells/mm² in the MP
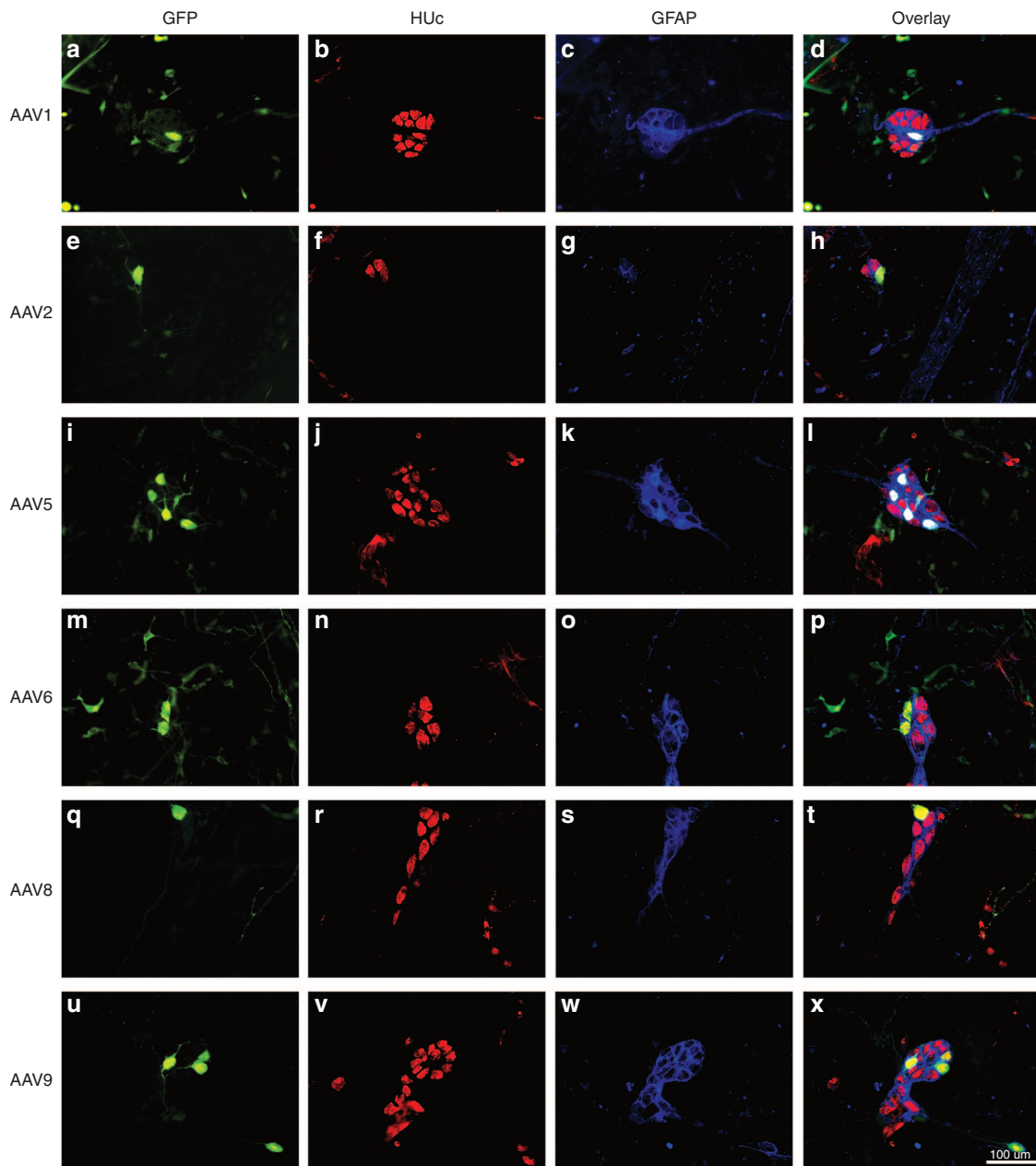
Figure 4 Neuronal tropism of recombinant adeno-associated virus (AAV) transduction in the submucosal plexus (SMP): serotypes 1, 2, 5, 6, 8, and 9. Adult male rats received direct injections of AAV (6 × 5 µl injections at 1.3×10^{12} vg/ml) into the wall of the descending colon and were sacrificed one month later, at which time the SMP was dissected. SMP tissue was stained for the neuronal marker HUc (red) and the enteric glia marker, glial fibrillary acidic protein (GFAP; blue). Following, the SMP was viewed under a fluorescent microscope and the transduction of neurons in the SMP was determined by examining the colocalization of green fluorescent protein (GFP; green) expression in HUc-positive cells (colocalization appears in yellow). Neuronal transduction was observed for all serotypes examined. Representative images of neuronal transduction are shown for AAV1 (**a–d**), AAV2 (**e–h**), AAV5 (**i–l**), AAV6 (**m–p**), AAV8 (**q–t**), and AAV9 (**u–x**). Scale bar in (**x**) represents 100 µm and applies to panels (**a–w**).

(**Supplementary Figure S1a,f**) and 3 ± 0.8 cells/mm² in the SMP (**Supplementary Figure S1g,l**), corresponding to $13.6 \pm 2.8\%$ and $15.5 \pm 8.8\%$ HUc-positive cells transduced in the MP and SMP, respectively (**Supplemnetary Figure S1b,h**).

The AAV8 capsid mutant vectors tested, AAV8-Y733F (**Supplementary Figure S2a–d,f,i**) and AAV8-doubleY-F+T-V (**Supplementary Figure S2a–d,g,j**), did not show any significant increases in transduction over WT AAV8 vector in either the MP (5 ± 2.9 cells/mm² and $20.7 \pm 6.1\%$ of HUc cells for AAV8-Y733F; 12.9 ± 7.3 cells/mm² and $25.2 \pm 15.3\%$ of HUc cells for

AAV8-doubleY-F+T-V) or SMP (4.2 ± 1 cells/mm² and $8.2 \pm 1.6\%$ of HUc cells for AAV8-Y733F; 14 ± 3.9 cells/mm² and $26.9 \pm 9.7\%$ of HUc cells for AAV8-doubleY-F+T-V).

Tropism of AAV transduction in the ENS

Next we wanted to determine what type of cells AAV was able to transduce within the ENS. Similar to the CNS, the ENS is composed mainly of neurons and glial cells.[1,2,8] To determine the phenotype of transduced cells, colonic tissue showing GFP-positive cells was stained for HUc, and also glial fibrillary acidic protein
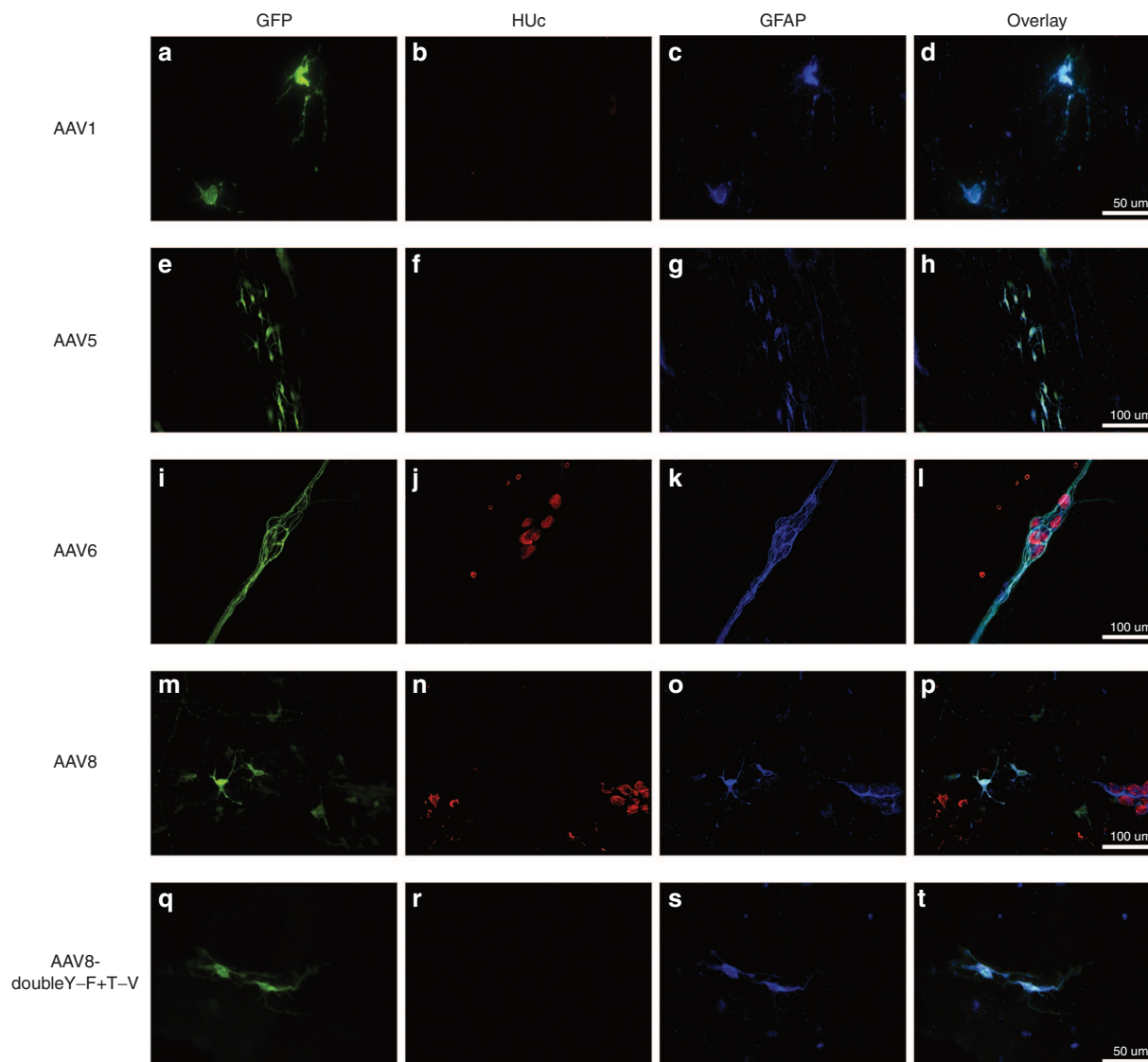
Figure 5 Glial tropism of recombinant adeno-associated virus (AAV) transduction. Adult male rats received direct injections of AAV (6 × 5 µl injections at $1.3 × 10^{12}$ vg/ml) into the wall of the descending colon and were sacrificed one month later, at which time the submucosal plexus (SMP) and myenteric plexus (MP) were dissected. MP and SMP tissue was stained for the enteric glia marker, glial fibrillary acidic protein (GFAP; blue). Following, tissue was viewed under a fluorescent microscope and the transduction of glia was determined by examining the colocalization of green fluorescent protein (GFP; green) expression in GFAP-positive enteric glia (colocalization appears turquoise). Micrographs also show the neuronal marker HUc (red). Glia transduction was rare and was only observed in AAV serotypes 1, 5, 6, 8 and AAV8-doubleY-F+T-V. AAV6 showed far more glial transduction than any other serotype. Morphologically, most glial transduction appeared to occur within reactive, protoplasmic or mucosal, enteric glia (**d,h,p, and t**). In contrast, AAV6 was able to transduce intraganglionic enteric glia (**l**). Representative images of glial transduction are shown for AAV1 in the MP (**a–d**), AAV5 in the MP (**e–h**), AAV6 in the SMP (**i–l**), AAV8 in the SMP (**m–p**), and AAV8-doubleY-F+T-V in the SMP (**q–t**). Scale bar in (**d,t**) represents 50 µm and applies to (**a–c**) and (**q–s**). Scale bars in (**h,l,p**) represent 100 µm and apply to (**e–g,i–k,m–o**).

(GFAP), a protein expressed in enteric glia. Similar to results observed in the CNS when using the same expression cassette, the vast majority of transduction mediated by all serotypes tested (with the exception of AAV6) was neuronal.[2,4,23,24] The MP exists in a relatively flat plane containing two-dimensional clusters of disc like neurons (**Figure 3** HUc; red), which are closely bundled by intraganglionic enteric glia (**Figure 3** GFAP; blue) along the edges of neurons. Transduction of neurons in the MP was seen in soma (**Figure 3a,e,i,m,q,u**) as well as the fibers tracts connecting ganglia (**Figure 3a,i,m**).

Neuronal transduction was also observed in the SMP (**Figure 4**). Unlike the MP, neurons within the SMP appear as

grape-like clustered that are sheathed in supportive intraganglionic enteric glia (see **Figure 4b–d**). Transduction appeared within soma (**Figure 4a,e,i,m,q,u**) as well as neuronal fibers (**Figure 4q,u**), however GFP-positive fibers in the SMP were not as abundant or intense as in the MP.

Similar to their WT counterparts, the AAV2 and 8 capsid mutants showed a highly neuronal tropism that was consistent across the MP (**Supplementary Figure S3**) and SMP (**Supplementary Figure S4**). We did not observe any changes in tropism produced by these capsid mutations.

Certain serotypes exhibited an exclusively neuronal tropism while others had a much more promiscuous tropism, showing
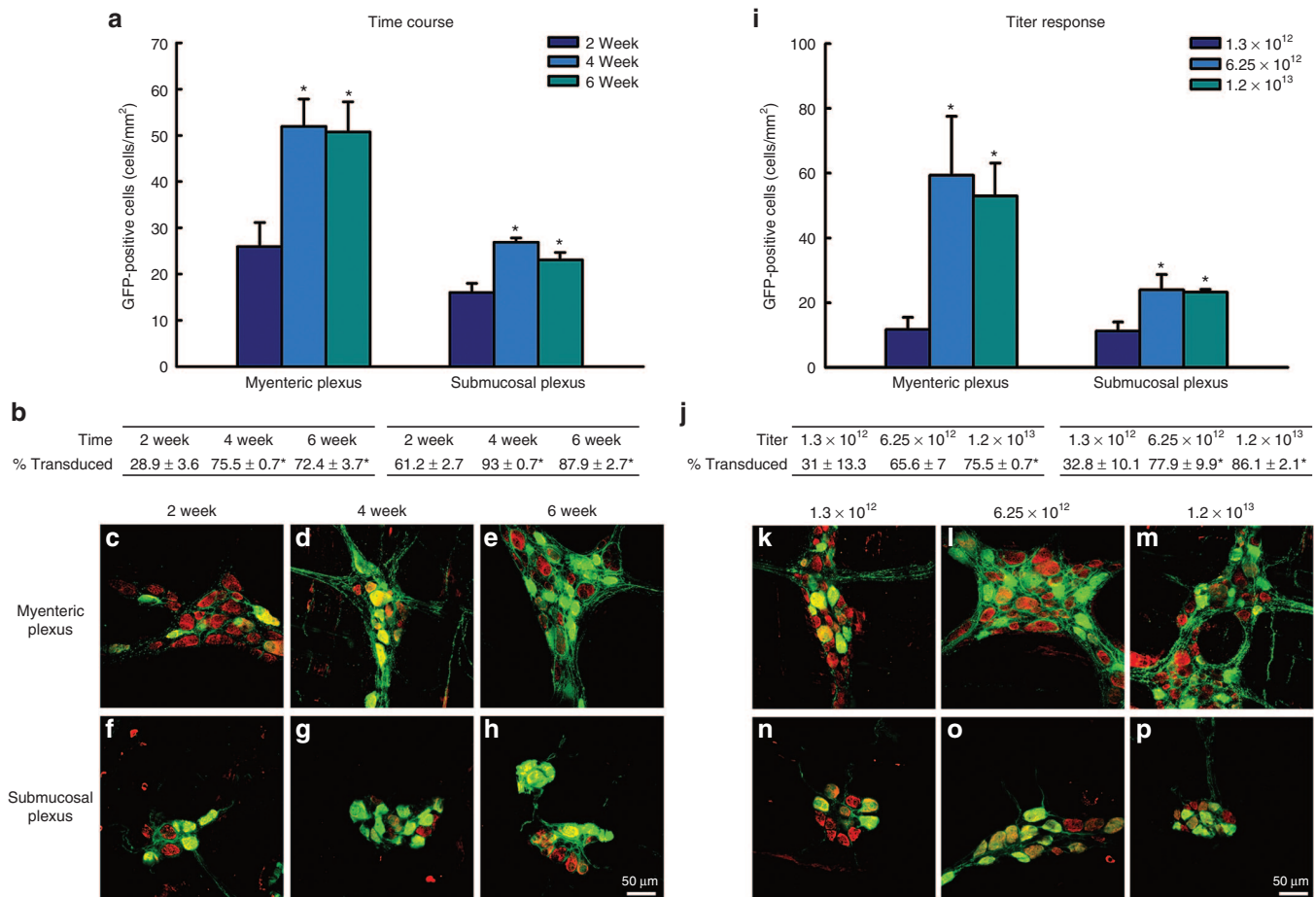
Figure 6 Time course and titer response of recombinant adeno-associated virus (AAV) serotype 9 in the myenteric plexus (MP) and submucosal plexus (SMP) of the enteric nervous system. Time course (**a–h**): Adult male rats received direct injections of high titer AAV9 (6×5 µl injections at 1.2×10^{13} vg/ml) into the wall of the descending colon and were sacrificed 2, 4, or 6 weeks postsurgery, at which time the MP and SMP were dissected and viewed under a fluorescent microscope. Transduction efficiency of the 2-week (**a**, dark blue columns), 4-week (**a**, light blue columns), and 6-week groups (**a**, turquoise columns) was measured by the quantification of green fluorescent protein (GFP) expressing cells in the MP (**a**, left column grouping) and SMP (**a**, right column grouping). Columns represent mean number of GFP-positive cells, expressed as cells/mm², + 1 SEM (n = 4–6/group). The 4- and 6-week groups had significantly more GFP-positive cells in both the MP and SMP than the 2-week group. No difference between the 4- and 6-week groups was observed. (**b**) The percent of HUc-positive cells expressing GFP ± SEM (n = 4–6/group). Representative images of GFP (green) and HUc (red) positive cells are shown for the 2-week (**c**), 4-week (**d**), and 6-week (**e**) group in the MP and the 2-week (**f**), 4-week (**g**), and 6-week (**h**) groups in the SMP. * Indicates significantly different than AAV9 at 2 weeks ($P < 0.05$). Titer response (**i–p**): Adult male rats received direct injections of AAV9 at a low titer (6×5 µl injections at 1.3×10^{12} vg/ml), an intermediate titer (6×5 µl injection at 6.25×10^{12} vg/ml) or a high titer (6×5 µl injections at 1.2×10^{13} vg/ml) into the wall of the descending colon and were sacrificed 1 month later, at which time the MP and SMP were dissected and viewed under a fluorescent microscope. Transduction efficiency of low-titer AAV9 (**i**, dark blue columns), intermediate titer AAV9 (**i**, light blue columns) and high-titer AAV9 (**i**, turquoise columns), were measured by the quantification of green fluorescent protein (GFP) expressing cells in the MP (**i**, left column grouping) and SMP (**i**, right column grouping). Columns represent mean number of GFP-positive cells, expressed as cells/mm², + 1 SEM (n = 4–6/group). The intermediate (6.25×10^{12}) and high titer (1.2×10^{13}) AAV9 groups had significantly more GFP-positive cells in both the MP and SMP than the low titer (1.3×10^{12}) AAV9 groups. (**j**) The percent of HUc-positive cells expressing GFP ± SEM (n = 4–6/group). Representative images of GFP (green) and HUc (red) positive cells are shown for the low titer (**k**), intermediate titer (**l**), and high titer (**m**) groups in the MP and the low titer (**n**), intermediate titer (**o**), and high titer (**p**) groups in the SMP. * Indicates significantly different than AAV9 at 1.2×10^{12} vg/ml ($P < 0.05$). Scale bar in (**h and g**) represents 100 µm and applies to all panels.

GFP expression within neurons as well as enteric glia. For example, AAV2 (**Figures 3e–h** and 4e–h) and AAV9 (**Figures 3u–x** and **4u–x**) exhibited an almost purely neuronal tropism. In contrast, AAV serotypes 1, 5, 6, 8 and AAV8-doubleY-F+T-V, showed both neuronal and glial transduction (**Figure 5**). It should be noted that in most instances glial transduction was proportionally secondary to neuronal transduction. However, special note should be paid to AAV6, which exhibited a tropism that was roughly equal between neurons and glia (**Figure 5i–l**). Further, a qualitative assessment of glial morphology suggested that the majority of glial transduction observed with other serotypes seemed to be taking place within reactive "protoplasmic" or "mucosal" enteric glia (**Figure 5d,h,p,t**). In contrast, while AAV6 also showed expression within reactive glia, it also transduced the structural intraganglionic enteric glia. This is well demonstrated in **Figure 5i–l**.

Time course and titer response of AAV9 transduction in the ENS

The ability of AAV to transduce cells of the ENS could have important implications to both model as well as potentially treat
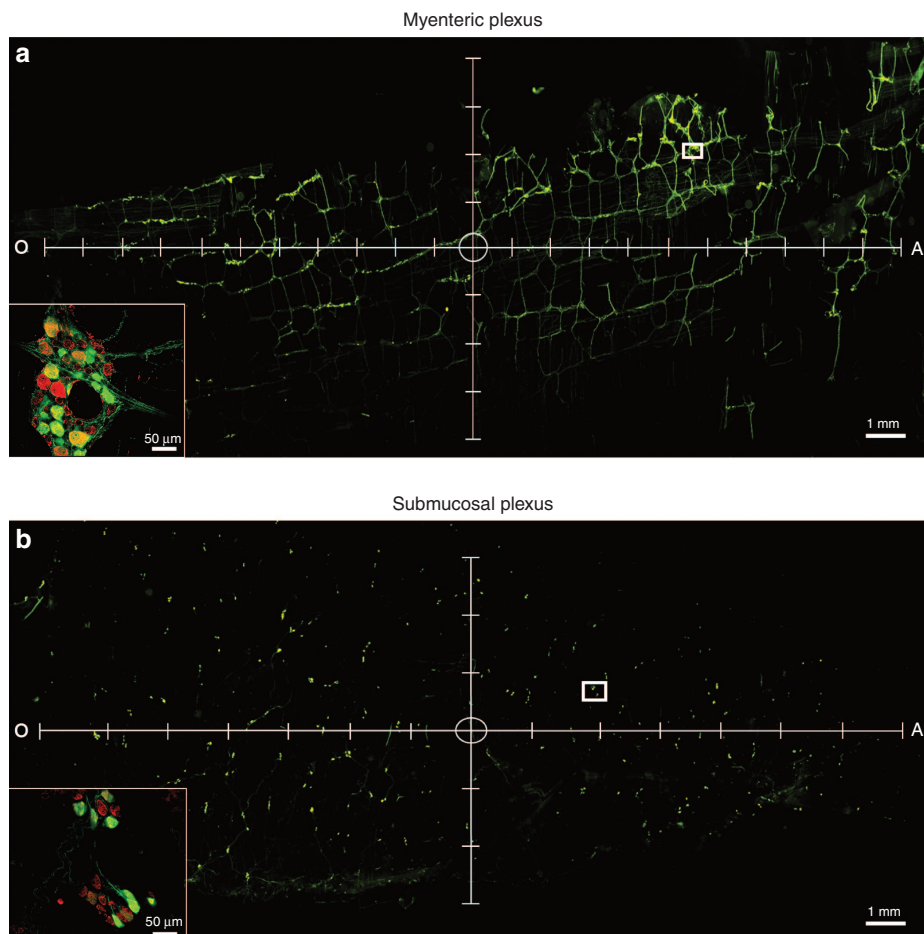
Figure 7 The spread of a single injection of recombinant adeno-associated virus (AAV) serotype 9 in the myenteric plexus (MP) and submucosal plexus (SMP) of the enteric nervous system. Adult male rats received direct injections of AAV9 (1.2×10^{13} vg/ml) into the wall of the descending colon and were sacrificed one month later, at which time the MP and SMP were dissected and viewed under a fluorescent microscope. The spread of transduction was determined by quantifying the area of the MP and SMP containing green fluorescent protein (GFP)-positive cells. Panel (**a**) and (**b**) show representative images of vector spread and transduction following a single injection of AAV9 within the MP and SMP, respectively. Representative images are shown with axis to indicate longitudinal (x-axis) and perpendicular (y-axis) spread. Tick marks on the axis represent 1 mm. The circle in the center of the axis represents the approximate location of the injection site. Insets represent high magnification images of the area within the white box in **a** and **b**. Scale bars in (**a**) and (**b**) represent 1 mm. Scale bars in the insets in (**a**) and (**b**) represent 50 µm.

disorders of the ENS. However, the level of transduction observed in our initial experiments was modest, which was not surprising given the relatively low titer utilized. Thus, we next wanted to determine if AAV transduction in the ENS could be increased in a titer-dependent manner, as well as to determine the optimal time postinjection needed for maximal transduction. In our initial experiments, AAV9 showed high levels of transduction and the most consistent neuronal transduction profile, thus we chose to perform a thorough characterization of the time course and titer response of AAV9 in both the MP and SMP.

To characterize the time course of AAV9 transduction, adult rats received identical injection of AAV9-GFP at a high titer of 1.2×10^{13} and GFP-positive cells were quantified in the MP and SMP at 2, 4, and 6 weeks postsurgery. Within both the MP and SMP, there was a significant increase in the number of GFP-positive cells/mm² from 2 weeks (25.9 ± 5.2 cells/mm² in the MP; **Figure 6a,c**; and 16 ± 2 cells/mm² in the SMP; **Figure 6a,f**) to 4 weeks postsurgery (51.8 ± 5.9 in the MP; **Figure 6a,d**; and 26.8 ± 0.9 cells/mm² in the SMP, **Figure 6a,g**). The percent of

HUc-positive cells transduced also increased from the 2 weeks postsurgery ($28.9 \pm 3.6\%$ in the MP; **Figure 6b,c**; and $61.2 \pm 2.7\%$ in the SMP; **Figure 6b,f**) to 4 weeks postsurgery ($75.5 \pm 0.7\%$ in the MP; **Figure 6b,d**; and $93 \pm 0.7\%$ in the SMP, **Figure 6b,g**). The level of transduction plateaued at 4 weeks postsurgery and there was no increase in transduction from 4 to 6 weeks postsurgery in either the MP (50.6 ± 6.5 cells/mm² and $72.4 \pm 3.7\%$ of HUc-positive cells; **Figure 6a,b,e**) or SMP (23 ± 1.6 cells/mm² and $87.9 \pm 2.7\%$ of HUc-positive cells; **Figure 6a,b,h**).

For the titer response, adult rats received identical injections of AAV9 at either the initial titer of 1.3×10^{12} vg/ml, an intermediate titer of 6.25×10^{12} vg/ml, or the high titer of 1.2×10^{13} vg/ml, and transduction in the MP and SMP was compared 1 month (when AAV9 reaches maximal expression in the MP and SMP) following surgery. As can be seen in **Figure 6i**, the intermediate titer of 6.25×10^{12} significantly increased transduction in the ENS compared to the low-titer group. AAV9 at 6.25×10^{12} produced an approximate fivefold increase in the number of GFP-positive cells in both the MP (59.3 ± 18.2 cells/mm²; **Figure 6i,l**)

and the SMP (23.9 ± 4.7 cells/mm^2; **Figure 6i,o**) over the lower titer injection (values given above; **Figure 6i,k,n**). The intermediate titer of 6.25×10^{12} also produced a significant increase in the percent of HUc-positive cells transduced in the MP ($65.6 \pm 0.7\%$; **Figure 6j,l**) and SMP ($77.9\% \pm 9.9$; **Figure 6j,o**) as compared to the low titer of 1.3×10^{12} (values given above; **Figure 6j,k,n**). The high titer of 1.2×10^{13} did not result in an increase in transduction over the intermediate titer group in either the MP (52.9 ± 10.1 cells/mm^2 and $75.5 \pm 0.7\%$ of HUc-positive cells; **Figure 6i,j,m**) or SMP (23.1 ± 0.8 cells/mm^2 and $86.1 \pm 2.1\%$ of HUc-positive cells; **Figure 6i,j,p**) suggesting a plateau in the number of transduced cells possible. In support of this notion, qPCR quantification of the relative changes in viral genome concentrations between treatment groups showed a titer-dependent increase in viral genomes detected from the low titer ($2^{\Delta\Delta Ct}$ of 5.7 ± 0.9 in the MP and 3.9 ± 0.2 in the SMP; **Supplementary Figure S5**), to the intermediate titer ($2^{\Delta\Delta Ct}$ of 18.7 ± 1.9 in the MP and 16.2 ± 4.3 in the SMP; **Supplementary Figure S5**), to high-titer group ($2^{\Delta\Delta Ct}$ of 72.5 ± 2.8 in the MP and 63.7 ± 3.9 in the SMP; **Supplementary Figure S5**), despite the absence of a corresponding increase in the number of cells/mm^2 or the percent of HUc-positive cells transduced (**Figure 6i,j**), implicating a saturation effect.

Spread of AAV transduction in the ENS

Future work will be aimed at modulating GI function using AAV-mediated gene delivery, thus, in the initial portion of this study, we aimed to target a relatively large portion of the colon (six injections spread out over ~1.5 cm^2 of the descending colon). However, to better understand the area of transduction that can be achieved by the current surgical administration, we also aimed to evaluate the spread of transduction following a single injection of AAV into the descending colon. Adult rats received a single injection of AAV9 (5 µl, 1.2×10^{13}vg/ml) into the wall of the descending colon and 1-month postsurgery the spread of transduction from the injection site was quantified. Following a single injection, the area containing GFP-positive cells was ~47.2 ± 1.8 mm^2 in the MP and 46.6 ± 5.5 mm^2 in the SMP. These values were back-calculated to correspond to the area of transduction within the unprocessed colon and thus represent the degree of spread that would be expected within an intact colon *in vivo*. **Figure 7** shows representative images of transduction spread following a single injection in the MP (**Figure 7a**) and the SMP (**Figure 7b**). The circle at the center of the axis represents the approximate location of the injection site. The majority of spread occurred along the longitudinal plane (oral to anal) of the ENS (**Figure 7a,b**, x-axis), although there was still a large amount of spread long the perpendicular plane (**Figure 7a,b**, y-axis).

In addition to measuring the spread of transduction following a single injection within the ENS, we also wanted to monitor any spread of transduction outside of the ENS. Vagal and sacral spinal parasympathetic nerves directly innervate the colon, and this innervation could serve as a potential route for spread of transduction outside of the ENS, possibly to the CNS. Accordingly, we monitored for transduction in the dorsal motor nucleus of the vagus and the lumbar/sacral region of the spinal cord following injection of AAV9 (6×5 µl, 1.2×10^{13} vg/ml) into the descending colon. We detected no GFP-positive cells (data not shown) or

viral genomes within either region (**Supplementary Figure S5**), suggesting that the observed transduction is limited to the area immediately surrounding the targeted ENS. In line with this, we did detect some GFP-positive cells within the smooth muscle of the injected gut wall, however the number of transduced smooth muscle cells was far lower compared to that observed within the ENS (data not shown). No transduction was observed in the mucosa of the injected colon.

Systemically delivered AAV readily transduces a multitude of organs throughout the body.[4,6,25,26] In order to address whether our surgical approach would result in viral particles in circulation, we also measured viral genomes of the liver and the spleen but detected no increase in genomes over naive control animals (**Supplementary Figure S5**).

Surgical adaptation

Many GI disorders are segmental in nature and localize to a specific area along the GI tract. Thus, we wanted to adapt the surgical delivery of AAV to other discrete areas along the GI tract. Adaptation of the surgical delivery was tested by performing a single injection of AAV9 (5 µl, 1.2×10^{13} vg/ml) directly into the wall of the small intestine, the cecum or the ascending colon of adult rats, and 1 month later the presence of GFP-positive cells in the ENS of the respective areas was probed. AAV9 transduced large networks of ganglia within the approximate area of the ileo-jejunual boundary within the small intestine (**Supplementary Figure S6a,b**). Further, targeted delivery of AAV9 transduced neurons in the cecum (**Supplementary Figure S6c**), and ascending colon (**Supplementary Figure S6d**), in a similar pattern to that observed in the descending colon.

We also wanted to translate our approach across species. The mouse is a commonly used organism to study GI function and many physiological analyses of GI function are performed in this species. As such, the ability of direct administration of AAV to transduce the murine ENS was analyzed. AAV9 (6×2 µl, 1.2×10^{13} vg/ml) was injected directly into the wall of the descending colon of adult mice, and 1 month later the presence of GFP-positive cells in the ENS was probed. **Supplementary Figure S6** demonstrates the ability of AAV9 to transduce neurons of the MP (**Supplementary Figure S6e**) and the SMP (**Supplementary Figure S6f**) within the mouse ENS, validating the ability to translate this approach across species.

Characterization of local inflammation in the ENS following AAV delivery

One limiting factor associated with viral vector-based gene therapy is the potential to elicit an immune response. In order to determine if the direct administration of AAV to the ENS results in an increase in local inflammation, immunohistochemical characterization of cells expressing ionized calcium-binding adapter molecule 1 (IBA1) was performed. IBA1 is a protein specific to macrophages and microglia, and is a common marker for neuroinflammation.[4,27] Although IBA1-positive cells are normally observed within neural tissue, an increase in IBA1-positive cell number, concurrent with morphological changes, is indicative of inflammation.[5,6,28] IBA1-positive cell numbers were quantified in the MP and SMP taken from representative AAV injected animals,

which showed successful transduction. Additionally, we analyzed changes in IBA1 cell numbers in animals injected with saline (control for vector administration), the proinflammatory endotoxin lipopolysaccharide (LPS; 6 × 5 µl, 1mg/ml; positive control), and animals that remained naïve to surgery (control for surgery).

Direct injection of LPS into the colon resulted in a significant increase in IBA1-positive cells in both the MP (**Supplementary Figure S7a,e**) and the SMP (**Supplementary Figure S7b,s**). Animals receiving injections of saline had similar numbers of IBA1-positive cells as naive animals (**Supplementary Figure S7a–d,q,r**). Finally, there were no significant changes in IBA1-positive cell numbers associated with any of the AAV serotypes tested (**Supplementary Figure S7a,b**).

In addition to quantifying changes in IBA1-positive cell numbers, we also performed a qualitative morphological assessment of IBA1-positive cells in all experimental groups. Resting macrophages are morphologically characterized by multiple processes extending from the soma in what is termed a "ramified" state.[8,29] Following an inflammatory stimulus, activated macrophage will begin to retract processes and take on a more amoeboid morphology.[9,29] In general, it appeared that IBA1-positive cells in the MP (**Supplementary Figure S7c,d,f–p**) more closely resembled resting macrophages than IBA1-positive cells in the SMP (**Supplementary Figure S7q,r**, T-DD), which seemed to have a rounder soma with shorter processes. LPS administration resulted in the appearance of amoeboid IBA1-positive cells, characteristic of local inflammation (**Supplementary Figure S7e,s**). In contrast, the noninjected animals showed IBA1-positive cells with long processes extending from a thin soma (**Supplementary Figure S7c,q**). There did not appear to be any large differences between the morphology of IBA1-positive cells between the noninjected and saline-treated animals, nor any of the serotypes tested within either the MP (**Supplementary Figure S7c,d,f–p**) or SMP (**Supplementary Figure S7q,r**, T-DD).

DISCUSSION

The use of AAV vectors to manipulate gene expression in various cell types within both central and peripheral tissue has been extensively characterized. However, to date, there are no reports on the targeted ability of AAV to transduce cells of the ENS within an adult animal. The work presented herein provides the first detailed description of the targeted use of AAV vectors to transduce both neurons and glia of the MP and SMP within delineated areas of the ENS.

One basic consideration when utilizing vector-based gene therapy is the optimal mode of gene delivery. Although systemic or peroral delivery of AAV has been shown to access the gut, these delivery methods must overcome significant barriers to achieve successful transduction, and dramatically increase the risk of off-target effects. For example, peroral administration of AAV can transduce cells of the gut mucosa, however via this route, AAV failed to transit the blood–gut epithelia barrier and transduce cells of the ENS.[5,10–13,30] Conversely, systemically delivered AAV can transit the blood–gut barrier, but will cross the blood–brain barrier and transduce cells of the CNS, as well as a wide range of other nontarget organ tissues throughout the body.[6,14,26,31,32] In contrast, using the method detailed herein, we did not observe any increase in viral genomes in any other tissues sampled, demonstrating highly efficient transduction that is limited to a discrete area of the ENS. By using direct injections of AAV into the wall of the descending colon, we were able to achieve transgene expression within both the MP and SMP within weeks after surgery. This approach allows for both spatial and temporal control of gene expression and could be further strengthened by the use of cell specific promoters in order to achieve transduction within a phenotypically distinct cell type; e.g., cholinergic neurons.

The approach used in the current study provides a unique platform upon which to model or treat ENS disorders. Due to the myriad of functions the ENS facilitates, and the severe ramifications of ENS dysfunction, it is becoming increasingly necessary to understand the physiology of the ENS in health and disease. The ability to manipulate gene expression specifically within the ENS obviates any off target effects that may arise when using the transgenic or psychological stress-based models that are currently used to study ENS disorders.[14–17] Moreover, targeted injections effectively circumvent any confound that may arise due to transduction of the brain or spinal cord following systemic injections. Additionally, we have shown that transduction of the ENS could also be achieved in both rat and mouse. Many of the physiological endpoints used to study ENS and GI function are performed in the mouse, and as such, the ability to manipulate gene expression within the murine ENS will undoubtedly prove to be an invaluable research tool. Further, this site-specific surgical approach enables transduction of a discrete functional unit within the ENS. Due to the fact that many disorders of the ENS localize to distinct areas along the GI tract, it is likely that this use of highly specific surgical injection of AAV will pave the way for model systems that more accurately recapitulate disorders of the ENS.

The level of transgene expression achieved by AAV is dependent upon the serotype, the expression cassette, and the target tissue. Here we aimed to determine the relative transduction efficiencies of various AAV serotypes within the cells of the ENS. AAV1 and AAV2 consistently showed very low levels of expression while AAV6 and AAV9 showed relatively high levels of expression. The increased transduction efficiency of AAV6 and AAV9 over other serotypes in the ENS is likely an effect of capsid interactions with cognate receptors. For example, the unique transduction efficiency and tropism of AAV6 may be due to a specific surface-exposed lysine residue. There are only six amino acid differences between AAV1 and AAV6, and of these, lysine 531 is responsible for the increased receptor binding, transduction efficiency and peripheral tropism of AAV6.[33,34] Similarly, the unique ability of AAV9 to penetrate epithelial barriers is thought to be mediated by a specific interaction with a unique receptor population.[19,20,31,32] Accordingly, the differential transduction efficiencies of the serotypes tested herein are indicative of unique capsid interaction with specific receptors in the ENS that favor AAV6 and AAV9.

Beyond transduction efficacy, we also sought to determine the tropism of the AAV serotypes tested. The ENS is composed of cells of both neuronal and glial lineage. All serotypes tested displayed at least some neuronal tropism. However, the fidelity of neuronal tropism varied, with some serotypes exhibiting almost purely neuronal transduction (e.g., AAV 2, 9) and others showing

promiscuous tropism, transducing both neurons and glia (*e.g.*, AAV6). AAV6 was remarkable in terms of glial tropism. AAV6 transduction of ENS glia could be seen in both reactive enteric glia as well as the structural intraganglionic glia, which compose a piece of the ganglionic infrastructure. Differential tropism of AAV6 as compared to other serotypes has been observed previously in other tissue such as liver, heart, and specific subregions of the CNS,[26,34–36] and may be a unique characteristic of the AAV6 capsid (*e.g.*, lysine 531). The impressive ability of AAV6 to transduce both glia and neurons, likely explains the high transduction efficiency of this serotype in this study. This non-neuronal transduction observed was rather surprising, however, as this event is relatively infrequent in the brain using the same viral genome and serotypes as utilized here.[23]

Within the current work AAV9 produced high levels of transduction with the most consistent neuronal tropism, thus, we sought to optimize the titer and time post-surgery necessary to produce the highest levels of transgene expression. AAV9 reached maximal transgene expression at 4 weeks, and at this 4-week time point AAV9-mediated transduction in both the MP and SMP plateaued at a titer of 6.25×10^{12} vg/ml. Although increasing titers beyond 6.25×10^{12} vg/ml increased the relative concentrations of AAV genomes detected within the injected area of the ENS, the percentage and number of neurons transduced remained constant at ~75% in the MP and 85% in the SMP, suggesting a ceiling effect in the number of neurons capable of being transduced. Indeed, in work by Gombash *et al.* [7], a slightly lower percentage of neuronal transduction was observed in the MP of neonatal mice after systemic delivery of AAV9. Within this work, it was demonstrated that excitatory, sensory, and ascending projection neurons were preferentially transduced, suggesting that an inability to transduce certain functional groups of neurons of the ENS, such as inhibitory neurons, is a possible limiting factor in the amount of transduction possible. Regardless, the fact that we observed an increase in viral genomes suggests that transgene expression can be increased using titers greater than 6.25×10^{12} vg/ml. This may be valuable when evaluating the titer-response to a certain gene, or when large amounts of gene-product are required.

Finally, a note must be made on the AAV-induced inflammation in the ENS. One inherent limitation to viral vector-based gene therapy is the potential to elicit an immune response. Injection of AAV can result in a humoral response, and the production of neutralizing antibodies, or a cell-mediated immune response and the destruction of virally infected host cells,[37] and as such represents a major obstacle that must be carefully monitored. Here, we monitored the initiation of a local immune response by examining the numbers and morphology of IBA1-positive cells within the transduced ENS. We found no increases in IBA1-positive cells in any of the AAV-injected animals. Further, the majority of IBA1-positive cells observed seemed to be in the "ramified" state, a morphology associated with inactive macrophages.[29] However, IBA1-positive cell numbers and morphology is a cursory analysis that is limited to local inflammation and yields no insight into a virally initiated humoral response. As such, future studies will aim to provide a more detailed analysis of any potential immune response by the targeted delivery of AAV to the ENS.

CONCLUSION

We have shown that targeted delivery of AAV vectors can successfully transduce cells of the ENS. Transduction was observed in both neurons and glia in the MP and the SMP. A comparison across serotypes revealed that AAV6 and AAV9 showed the highest levels of transduction. We observed differential tropism based upon the serotype being used, with AAV9 primarily transducing neurons and AAV6 transducing neurons and glia. Transduction efficiency of AAV9 scaled with titer and time, and plateaued at 4 weeks postsurgery with a titer of 6.25×10^{12} vg/ml. Infection produced little to no local immune response specific to the vector. The spread from a single, targeted injection of AAV9 into the descending colon covered an area of ~47 mm² and no viral genomes were detected in other tissues. Finally, the targeted application of AAV was also translated to the small intestine, the proximal colon, and the murine ENS. To our knowledge, this is the first detailed report on the ability of targeted AAV delivery to transduce both neurons and glia within predefined areas of the ENS of an adult animal. This study illustrates that various AAV serotypes can be used to successfully transduce relatively specific cell types within discrete regions of the ENS, opening the door for the creation of more accurate models of ENS dysfunction as well as the potential for the development of therapeutic applications.

MATERIALS AND METHODS

AAV vector construction. AAV vectors encoding humanized GFP under control of the hybrid chicken β-actin/cytomegalovirus promoter were produced as described previously.[33] Briefly, viruses were created by cotransfection of the AAV transgene plasmids with a helper plasmid encoding capsid proteins for serotypes AAV1, AAV2, AAV5, AAV6, AAV8, or AAV9. Subsets of AAV2- and AAV8-based vectors were produced by cotransfection with respective helper plasmids encoding capsids containing point mutations of surface exposed tyrosine residues (tyrosine to phenylalanine, Y-F). These included AAV2-Y444F, AAV2-Y444F+Y500F+Y703F (referred to as AAV2-tripleY-F), and AAV8-Y733F.[19,20] An additional subset of vectors tested contained a combination of Y-F and threonine-valine (T-V) capsid mutations These included AAV2-tripleY-F+T491V (referred to as AAV2-tripleY-F+T-V) and AAV8-Y447F+Y733F+T494V (referred to as AAV8-doubleY-F+T-V).[18,22] These capsid mutants exhibit increased transduction efficiency in other tissues.[18–22] Following transfection, cells were harvested and lysed, and virus was purified as described previously.[33,38] Virus titers were determined using dot blot assays[33] and all viral preparations were normalized to 1.3×10^{12} viral genomes per milliliter (vg/ml) using balanced salt solution (Alcon Laboratories, Fort Worth, TX), with the exception of the high titer AAV9, which was normalized to 1.2×10^{13} vg/ml.

Animals and surgery. Experiments were conducted on young adult (220 g) male Sprague Dawley rats or young adult (30 g) C57Bl/6j mice in accordance with guidelines of the Michigan State University Institutional Animal Care & Use Committee (AUF 08/12-150-00). Rats were housed two per cage, while mice were housed four to five per cage, and maintained in a light-controlled (12 hours light/dark cycle; lights on 06:00 hours) and temperature-controlled (22 ± 1 °C) room, and provided with food and tap water *ad libitum*.

All surgery was performed under 2% isofluorane anesthesia. The surgical site was shaved and scrubbed with betadine. A vertical incision was made in the abdomen from the level of the pelvis to the sternum. The abdominal wall was resected exposing the peritoneal cavity after which the descending colon was exposed. A small horizontal tattoo (AIMS tattoo ink) was placed midway down the descending branch of

the colon in order to mark the injection site. Following, rats received 6×5 µl injections, and mice received 6×2 µl injections, of AAV applied in a 2×3 injection grid distal to the tattoo. Initial experiments were performed in order to optimize the delivery parameters of AAV to the ENS (**Supplementary Table S1**) and the final optimized parameters are described below. The number and volume of injections was chosen to ensure that the spread of virus covered an area large enough to allow for analyses of transduction efficiency and tropism. A subset of rats received a single 5 µl injection in order to determine the degree of vector spread achieved from a single injection and demonstrate transduction in distinct regions of the ENS. Injections into the wall of the descending colon were made horizontally to the longitudinal axis of the colon, with the bevel of the needle resting in between the muscle layers, just below the level of the tattoo, using a siliconized (sigmacote, Sigma, St. Louis, MO) 50 µl Hamilton syringe with a 22 gauge (rat) or 31 gauge (mouse) beveled needle, connected to a Harvard Apparatus foot operated pump. AAV was injected at a flow rate of 10 µl/minute in order to enhance convection, and afterward the needle was left in place for 1 minute to prevent reflux.

Following injections, the contents of the peritoneal cavity were put back in place, the abdominal wall was sutured and the overlying skin was stapled closed. Animals were given an injection of timentin (60 mg/kg; i.p.) and ketofen (5 mg/kg; i.p.) in order to prevent infection and reduce discomfort. Animals were monitored postoperatively for signs of distress or infection.

Tissue collection. At the time of sacrifice, animals received a lethal injection of sodium pentobarbital and were transcardially perfused with 0.9% sterile saline. Brains and spinal cords were rapidly removed and postfixed in 4% paraformaldehyde in phosphate-buffered saline (PBS) for 3 days. The liver and spleen was removed and immediately frozen. The descending colon (cut ~1 cm above and 2 cm below the level of the tattoo) was collected. After removal from the animal, the collected colon tissue was cut along the longitudinal axis, stretched, and pinned out on a gelatin-coated petri dish. The colon tissue was then washed three times with PBS and postfixed in 4% paraformaldehyde in PBS for 24 hours. The descending colon tissue (at the level of the injection) was cut into $0.5\,cm^2$ sections. The submucosal plexus and myenteric plexus was then dissected from these sections under a dissecting microscope and stored in TBS at 4 °C until further histological processing.

Immunohistochemistry. For colonic tissue, immunohistochemistry was performed on free floating sections containing the submucosal and myenteric plexus, respectively. Sections were washed in 1× TBS containing 0.25% Triton x-100, blocked in 10% serum (specific to the secondary antibody) and incubated for 3 days in primary antibody at 4 °C. Primary antibodies used were rabbit anti-GFP (Abcam; ab290, Cambridge, MA), chicken anti-GFAP (Abcam; ab4674), mouse anti-HUc/HUd (Life Technologies; A21271), rabbit anti-IBA1 (Wako; PDF3116, Richmond, VA). Secondary antibodies used were Goat anti-mouse alexafluor 594 (Life Technologies; A11005), goat anti-rabbit alexafluor 488 (Life Technologies; A11008, Carlsbad, CA), donkey anti-chicken IRDye 680LT (LiCor; 926–68028, Lincoln, NE). Sections were then washed in TBS and covered slipped using vectashield hard set mounting medium.

For brain tissue and spinal cords, tissues were frozen on dry ice and coronal sections (40 µm) were cut through the rostrocaudal axis of the brain using a sliding stage microtome. Immunohistochemistry was performed on free-floating sections. Sections were washed in 1× TBS containing 0.25% Triton x-100, blocked in 10% normal goat serum and incubated overnight in rabbit anti-GFP (Abcam; ab290) primary antibody at 4 °C. Sections were then washed and incubated in biotin-conjugated goat anti-rabbit (Millipore; AP132B, Billerica, MA), followed by 2 hours in ABC solution (Vector Labs Burlingame, CA). Sections were then incubated in diaminobenzidine (50 mg/100 ml with 0.03% hydrogen peroxide). Finally, sections were washed in TBS and covered slipped using cytoseal mounting medium (Thermo scientific, Kalamazoo, MI.).

Tissue was viewed on a Nikon eclipse 90i fluorescence microscope connected to a Q-imaging fast 1394 camera.

Cell counts. GFP-positive cell counts were performed as previously described.[39] Briefly, tissue collected from the same location relative to the tattoo for all animals from each respective serotype grouping was analyzed. $5\,mm^2$ sections of tissue from an area immediate to the injection site as well as sections anterior and posterior to the injection site were viewed under a fluorescence microscope for native fluorescence of the reporter gene or immunofluorsecence of HUc-positive neurons, and images of the respective area of colon were acquired. The exposure time used to acquire all images was identical. GFP- and HUc-positive cell counts in the MP and SMP were performed from the acquired images. Following, GFP- and HUc-positive cell counts from the immediate, anterior, and posterior sections were pooled in order to get a total GFP- and HUc-positive cell number for all animals. Total GFP cell counts were then normalized to tissue area and expressed as $cells/mm^2$ or represented as the percentage of HUc-positive neurons within the same counting area. Within initial experiments, there were some failed injection of AAV to the ENS and these animals were excluded from further analysis.

qPCR analysis of AAV genomes. Genomic DNA was extracted from the previously dissected MP and SMP by incubating tissue in extraction buffer (200 mmol/l tris, 250 mmol/l NaCl, 25 mmol/l ethylenediaminetetraacetic acid, 0.5% sodium dodecyl sulfate) with proteinase K and RNase A at 55 °C followed by phenol/chloroform extraction and ethanol precipitation of the DNA. DNA concentration was determined using a Nanodrop. qPCR primers for the AAV genome (Integrated DNA technology, Coralville, IA) and glyceraldehyde 3-phosphate dehydrogenase (Applied Biosystems, Waltham, MA) were conjugated to a FAM or VIC reporter, respectively. All primers were ensured to produce a single product as assessed by melt curve analysis. Glyceraldehyde 3-phosphate dehydrogenase was used as the reference gene and detection was similar across treatment groups. Samples for PCR reactions were run in quadruplicate and averaged to give a single mean value per sample. Changes between treatment groups were analyzed by the differences in ΔC_t, which compares the C_t value of the AAV genome to that of the glyceraldehyde 3-phosphate dehydrogenase control gene. Data is presented as fold change over corresponding control tissue as determined by the $\Delta\Delta C_t$, which represent the ΔC_t normalized to a calibrator, in this case noninjected control tissue.

Statistical analysis. The experimenter was blind to all experimental conditions during data collection and analysis. One-way analysis of variance tests were used to test for statistical significance between two or more groups with a single independent variable. A *P* value of less than or equal to 0.05 was considered statistically significant. If the analysis of variance revealed an interaction of statistical significance, *post hoc* analysis was followed by between group comparisons using Tukey's test.

SUPPLEMENTARY MATERIAL
Figure S1. Transduction efficiency of recombinant adeno–associated virus (AAV) serotype 2 capsid mutants in the myenteric plexus (MP) and submucosal plexus (SMP) of the enteric nervous system.
Figure S2. Transduction efficiency of recombinant adeno–associated virus (AAV) serotype 8 capsid mutants in the myenteric plexus (MP) and submucosal plexus (SMP) of the enteric nervous system.
Figure S3. Neuronal tropism of recombinant adeno–associated virus (AAV) transduction in the myenteric plexus (MP): AAV serotypes 2 and 8 capsid mutants.
Figure S4. Neuronal tropism of recombinant adeno–associated virus (AAV) transduction in the submucosal plexus (SMP): AAV serotypes 2 and 8 capsid mutants.
Figure S5. Quantification of AAV spread and titer–dependent changes in viral genomes within the myenteric plexus (MP) and submucosal plexus (SMP).
Figure S6. Targeted delivery of AAV9 to the ENS within the rat small intestine, the rat proximal colon, and the mouse colon.
Figure S7. Local inflammation induced by the targeted delivery of

the recombinant adeno-associated virus (AAV) to the myenteric plexus (MP) anf submucosal plexes (SMP) of the enteric nervous system.

Table S1. Optimization of gene delivery to the enteric nervous system.

REFERENCES

1. Daya, S and Berns, KI (2008). Gene therapy using adeno-associated virus vectors. *Clin Microbiol Rev* **21**: 583–593.
2. Flotte, TR (2004). Gene therapy progress and prospects: recombinant adeno-associated virus (rAAV) vectors. *Gene Ther* **11**: 805–810.
3. Mueller, C and Flotte, TR (2008). Clinical gene therapy using recombinant adeno-associated virus vectors. *Gene Ther* **15**: 858–863.
4. Mingozzi, F and High, KA (2011). Therapeutic *in vivo* gene transfer for genetic disease using AAV: progress and challenges. *Nat Rev Genet* **12**: 341–355.
5. During, MJ, Xu, R, Young, D, Kaplitt, MG, Sherwin, RS and Leone, P (1998). Peroral gene therapy of lactose intolerance using an adeno-associated virus vector. *Nat Med* **4**: 1131–1135.
6. Fu, H, Dirosario, J, Killedar, S, Zaraspe, K and McCarty, DM (2011). Correction of neurological disease of mucopolysaccharidosis IIIB in adult mice by rAAV9 trans-blood-brain barrier gene delivery. *Mol Ther* **19**: 1025–1033.
7. Gombash, SE, Cowley, CJ, Fitzgerald, JA, Hall, JC, Mueller, C, Christofi, FL *et al.* (2014). Intravenous AAV9 efficiently transduces myenteric neurons in neonate and juvenile mice. *Front Mol Neurosci* **7**: 81.
8. Wood, JD. *Enteric Nervous System (The-Brain-In-The-Gut).* Morgan & Claypool Life Sciences, Princeton, NJ. 2011.
9. Belkind-Gerson, J, Graeme-Cook, F and Winter, H (2006). Enteric nervous system disease and recovery, plasticity, and regeneration. *J Pediatr Gastroenterol Nutr* **42**: 343–350.
10. Forsyth, CB, Shannon, KM, Kordower, JH, Voigt, RM, Shaikh, M, Jaglin, JA *et al.* (2011). Increased intestinal permeability correlates with sigmoid mucosa alpha-synuclein staining and endotoxin exposure markers in early Parkinson's disease. *PLoS One* **6**: e28032.
11. Braak, H, de Vos, RA, Bohl, J and Del Tredici, K (2006). Gastric alpha-synuclein immunoreactive inclusions in Meissner's and Auerbach's plexuses in cases staged for Parkinson's disease-related brain pathology. *Neurosci Lett* **396**: 67–72.
12. Shannon, KM, Keshavarzian, A, Dodiya, HB, Jakate, S and Kordower, JH (2012). Is alpha-synuclein in the colon a biomarker for premotor Parkinson's disease? Evidence from 3 cases. *Mov Disord* **27**: 716–719.
13. Shannon, KM, Keshavarzian, A, Mutlu, E, Dodiya, HB, Daian, D, Jaglin, JA *et al.* (2012). Alpha-synuclein in colonic submucosa in early untreated Parkinson's disease. *Mov Disord* **27**: 709–715.
14. Mayer, EA and Collins, SM (2002). Evolving pathophysiologic models of functional gastrointestinal disorders. *Gastroenterology* **122**: 2032–2048.
15. Dawson, TM, Ko, HS and Dawson, VL (2010). Genetic animal models of Parkinson's disease. *Neuron* **66**: 646–661.
16. Kanaan, NM and Manfredsson, FP (2012). Loss of functional alpha-synuclein: a toxic event in Parkinson's disease? *J Parkinsons Dis* **2**: 249–267.
17. Kuhn, M, Haebig, K, Bonin, M, Ninkina, N, Buchman, VL, Poths, S *et al.* (2007). Whole genome expression analyses of single- and double-knock-out mice implicate partially overlapping functions of alpha- and gamma-synuclein. *Neurogenetics* **8**: 71–81.
18. Kay, CN, Ryals, RC, Aslanidi, GV, Min, SH, Ruan, Q, Sun, J *et al.* (2013). Targeting photoreceptors via intravitreal delivery using novel, capsid-mutated AAV vectors. *PLoS One* **8**: e62097.
19. Petrs-Silva, H, Dinculescu, A, Li, Q, Min, SH, Chiodo, V, Pang, JJ *et al.* (2009). High-efficiency transduction of the mouse retina by tyrosine-mutant AAV serotype vectors. *Mol Ther* **17**: 463–471.
20. Petrs-Silva, H, Dinculescu, A, Li, Q, Deng, WT, Pang, JJ, Min, SH *et al.* (2011). Novel properties of tyrosine-mutant AAV2 vectors in the mouse retina. *Mol Ther* **19**: 293–301.
21. Aslanidi, GV, River, AE, Ortiz, L, Song, L, Ling, C, Govindasamy, L et al. (2013). Small, N-terminal tags activate Parkin E3 ubiquitin ligase activity by disrupting its autoinhibited conformation. *PLoS One* **8**: e59142–e59142.
22. Gabriel, N, Hareendran, S, Sen, D, Gadkari, RA, Sudha, G, Selot, R et al. (2013). Bioengineering of AAV2 capsid at specific serine, threonine, or lysine residues improves its transduction efficiency *in vitro* and in vivo. *Hum Gene Ther Methods* **24**: 80–93.
23. Burger, C. (2004). Recombinant AAV viral vectors pseudotyped with viral capsids from serotypes 1, 2, and 5 display differential efficiency and cell tropism after delivery to different regions of the central nervous system. *Mol Ther* **10**: 302–317.
24. Reimsnider, S, Manfredsson, FP, Muzyczka, N and Mandel, RJ (2007). Time course of transgene expression after intrastriatal pseudotyped rAAV2/1, rAAV2/2, rAAV2/5, and rAAV2/8 transduction in the rat. *Mol Ther* **15**: 1504–1511.
25. Inagaki, K, Fuess, S, Storm, TA, Gibson, GA, Mctiernan, CF, Kay, MA *et al.* (2006). Robust systemic transduction with AAV9 vectors in mice: efficient global cardiac gene transfer superior to that of AAV8. *Mol Ther* **14**: 45–53.
26. Zincarelli, C, Soltys, S, Rengo, G and Rabinowitz, JE (2008). Analysis of AAV serotypes 1-9 mediated gene expression and tropism in mice after systemic injection. *Mol Ther* **16**: 1073–1080.
27. Ito, D, Tanaka, K, Suzuki, S, Dembo, T and Fukuuchi, Y (2001). Enhanced expression of Iba1, ionized calcium-binding adapter molecule 1, after transient focal cerebral ischemia in rat brain. *Stroke* **32**: 1208–1215.
28. Qin, L, Wu, X, Block, ML, Liu, Y, Breese, GR, Hong, JS *et al.* (2007). Systemic LPS causes chronic neuroinflammation and progressive neurodegeneration. *Glia* **55**: 453–462.
29. Streit, WJ, Walter, SA and Pennell, NA (1999). Reactive microgliosis. *Prog Neurobiol* **57**: 563–581.
30. During, MJ, Symes, CW, Lawlor, PA, Lin, J, Dunning, J, Fitzsimons, HL *et al.* (2000). An oral vaccine against NMDAR1 with efficacy in experimental stroke and epilepsy. *Science* **287**: 1453–1460.
31. Manfredsson, FP, Rising, AC and Mandel, RJ (2009). AAV9: a potential blood-brain barrier buster. *Mol Ther* **17**: 403–405.
32. Foust, KD, Nurre, E, Montgomery, CL, Hernandez, A, Chan, CM and Kaspar, BK (2009). Intravascular AAV9 preferentially targets neonatal neurons and adult astrocytes. *Nat Biotechnol* **27**: 59–65.
33. Zolotukhin, S, Potter, M, Zolotukhin, I, Sakai, Y, Loiler, S, Fraites, TJ Jr *et al.* (2002). Production and purification of serotype 1, 2, and 5 recombinant adeno-associated viral vectors. *Methods* **28**: 158–167.
34. Wu, Z, Asokan, A, Grieger, JC, Govindasamy, L, Agbandje-McKenna, M and Samulski, RJ (2006). Single amino acid changes can influence titer, heparin binding, and tissue tropism in different adeno-associated virus serotypes. *J Virol* **80**: 11393–11397.
35. Manfredsson, FP, Burger, C, Sullivan, LF, Muzyczka, N, Lewin, AS and Mandel, RJ (2007). rAAV-mediated nigral human parkin over-expression partially ameliorates motor deficits via enhanced dopamine neurotransmission in a rat model of Parkinson's disease. *Exp Neurol* **207**: 289–301.
36. Aschauer, DF, Kreuz, S and Rumpel, S (2013). Analysis of transduction efficiency, tropism and axonal transport of AAV serotypes 1, 2, 5, 6, 8 and 9 in the mouse brain. *PLoS One* **8**: e76310.
37. Zaiss, AK and Muruve, DA (2005). Immune responses to adeno-associated virus vectors. *Curr Gene Ther* **5**: 323–331.
38. Jacobson, SG, Acland, GM, Aguirre, GD, Aleman, TS, Schwartz, SB, Cideciyan, AV *et al.* (2006). Safety of recombinant adeno-associated virus type 2-RPE65 vector delivered by ocular subretinal injection. *Mol Ther* **13**: 1074–1084.
39. Patel, BA, Dai, X, Burda, JE, Zhao, H, Swain, GM, Galligan, JJ *et al.* (2010). Inhibitory neuromuscular transmission to ileal longitudinal muscle predominates in neonatal guinea pigs. *Neurogastroenterol Motil* **22**: 909–18, e236.